Limitations of Inductive Circuit Model Representations of Meander Line Antennas

Steven R. Best*
AFRL/SNHA
80 Scott Drive
Hanscom AFB, MA 01731
srbest@att.net

Jarrett D. Morrow
Cushcraft Corporation
48 Perimeter Road
Manchester, NH 03103
jarrettm@cushcraft.com

Abstract: The resonant frequency of meander line antennas can be predicted using an equivalent inductor circuit model representation. As a function of increasing number of meander sections, these models provide a reasonable approximation of the relative change in resonant frequency. Here, some limitations of these inductor circuit model representations are examined for different meander line antennas having a fixed number of meander sections. These limitations are explained in a broad sense in terms of the equivalent circuit parameters of the meander line geometry.

1. Introduction

The resonant frequency of the simple meander line antenna [1]-[3] is typically modeled using an equivalent inductor circuit model representation [1]. In these representations, each meander line section is modeled as an equivalent inductor. Adding the total equivalent inductance of the meander line sections to the self-inductance of the straight wire, the resonant frequency of the meander line can be approximated relative to that of the straight monopole antenna of the same height. For an increasing number of meander sections, these circuit model representations provide a reasonable approximation of the meander line's resonant frequency.

Here, the inductor circuit model representation of the meander line antenna is applied to several meander lines configurations where changes are implemented in the meander geometry in terms of the meander section length and spacing. In these cases, it is demonstrated that the inductor circuit model representations are not adequate in predicting the relative change in resonant frequency of these antennas. The limitations of the inductor circuit model are explained in general terms as a function of the effective circuit model behavior of these antennas. A full circuit model of the meander line antenna is not presented at this time, as it is focus of ongoing work.

2. The Meander Line Antenna

Consider the family of meander line monopole antennas illustrated in Fig. 1. In these antennas, the number of meander sections is sequentially increased from 0 to 5. These antennas have an overall height of 10 cm and a wire diameter of 0.5 mm. As the number of meander sections increases, the total effective self-inductance of the wire increases and the resonant frequency of the antenna decreases accordingly.

The self-resonant frequency of the straight monopole antenna can be related to its equivalent self-inductance as follows, presuming that the monopole is self-resonant when its, h, is approximately $0.24\,\lambda$ [1].

0-7803-7846-6/03/$17.00 ©2003 IEEE

$$L_S = \frac{\mu}{\pi} 0.2384\,\lambda \left(\ln\left(4\,\frac{0.2384\,\lambda}{d}\right) - 1\right) \tag{1}$$

where L_S is the equivalent self-inductance of the monopole, d is the monopole wire diameter and λ is the monopole's resonant wavelength. The resonant frequency of the meander line antennas can be approximated using an inductor circuit model representation, where each meander section is modeled as an equivalent inductor as shown in Fig. 2. The inductance of each meander section is determined from an equivalent transmission line model where the characteristic impedance of each meander section given as

$$Z_O = 276 \log\left(\frac{2\,s}{d}\right) \tag{2}$$

where s is the spacing of the meander section. The equivalent inductance of each section, L_M, is then determined from the input impedance of each section as follows

$$L_M = \frac{|Z_O \tanh(\gamma l)|}{\omega} \tag{3}$$

where γ is the free space propagation factor, l is the length of the meander section and ω is simply the radian frequency. The resonant frequency of the meander line antenna having the same height as the monopole antenna, h, is then determined from the solution for resonant frequency in Eq. (1) where the inductance L_S, is replaced by the sum of $L_S + N\,L_M$, where N is the number of meander sections.

3. Resonant Frequency Behavior of the Meander Line Antenna

The resonant frequencies of the meander line antennas shown in Fig. 1 were determined using the NEC 4 engine of EZNEC Pro [4]. The M0 configuration is self-resonant at 714.7 MHz, while the M5 configuration is self-resonant at 371.3 MHz. The resonant frequency of these meander lines was also approximated using the equivalent inductor circuit model equations described above as well as using an equivalent NEC model, where each meander line section in the antenna is replaced with an equivalent inductor load. For the antennas depicted in Fig. 1, s is equal to 1 cm, while l is equal to 2 cm. Using Eqs. (2) and (3), the value of L_M was determined to be 0.02865 μH. A comparison of the resonant frequencies as a function of increasing number of meander sections is presented in Fig. 3.

From Fig. 3, it is evident that the equivalent inductor models of the meander line antenna provide a reasonable approximation of its resonant frequency. However, it is important to note that the equivalent inductor model (Eqs. (1) – (3)) predicts a linear decrease in resonant as a function of increasing meander sections. The actual resonant frequency of the meander line antenna will not diminish linearly with increasing number of meander sections.

In examining the limitations of the inductor circuit model representation of the meander line antenna, some of its physical properties are varied and the relative change in resonant frequency is examined. First, the single meander section antenna, the M1 configuration, is considered where the meander spacing s, is varied from 0.25 cm to 5 cm. The resonant frequency behavior of this antenna as a function of meander spacing, predicted using the different models, is presented in Fig. 4. While the absolute resonant frequency predictions using Eqs. (1) – (3) and the NEC inductor load model are not precise they do provide a reasonable estimate of the relative change in resonant frequency.

Next, the M2 meander line configuration is considered where the separation between the meander sections is varied from 0.25 cm to 4 cm. The resonant frequency behavior as a function of meander section separation is presented in Fig 5. In this case, the equivalent inductor model of the meander line antenna (Eqs. (1) – (3)), does not provide a reasonable prediction of the relative change in resonant frequency. This simple equivalent inductor model representation offers no capability to account for the change in meander spacing. Similar comments are also valid for the NEC inductor load model of the meander line antenna.

Finally, the orientation of alternate meander sections is reversed as shown in Fig. 6 to examine the effects of changing the physical meander layout. The resonant frequency behavior as a function of reversing the meander section orientation is presented in Fig 7. In this case, the resonant frequency of the meander line antennas does not change significantly. However, the equivalent inductor model of the meander line antenna (Eqs. (1) – (3)) does not have the capability to account for the change in meander orientation. Similar comments are also valid for the NEC inductor load model of the meander line antenna.

4. Discussion

The simple inductive circuit model representations of the meander line antenna predict the resonant frequency of the antenna as a function of the equivalent self-inductance of each meander section. These models provide a reasonable approximation of the meander line antenna's resonant frequency as a function of increasing number of meander sections, however, they do not offer the flexibility to account for changes in the meander line configuration such as changes in the spacing between meander sections or a reversal of the meander section orientation.

The principle features that these inductive circuit model representations lack is the ability to account for the self-capacitance of each meander line section and the mutual capacitance between meander line sections. Not being able to account for the self-capacitance of each meander line section results in an inaccuracy in the calculated value of the meander section's self-inductance. This results in a minor lack of precision in the predicted resonant frequency value. Not being able to account for the mutual capacitance between meander sections, causes an inaccuracy in the resonant frequency prediction as a function of meander section spacing. Additionally, it causes the predicted change in resonant frequency as a function of increasing number of meander sections to diminish linearly, when in fact it does not.

Because of these fundamental limitations associated with inductive circuit model representations, a complete circuit model of the meander line antenna is being developed to account for the self-capacitance of each meander section and the mutual capacitance between meander sections.

6. References

[1] T. Endo, Y. Sunahara, S. Satoh and T. Katagi, "Resonant Frequency and Radiation Efficiency of Meander Line Antennas," Electronics and Communications in Japan, Part 2, Vol. 83, No. 1, 2000.

[2] T. J. Warnagirism and T. J. Minardo, "Performance of a Meandered Line as an Electrically Small Transmitting Antenna," IEEE Trans. Antennas Propagat., Vol. 46, pp. 1797-1801, Dec. 1998.

[3] K. Fujimoto *et al*, "Small Antennas," Research Studies Press, England; John Wiley and Sons, New York, 1987.

[4] EZNEC/4 Antenna Modeling Software, Roy Lewallen, P.E., http://www.eznec.com.

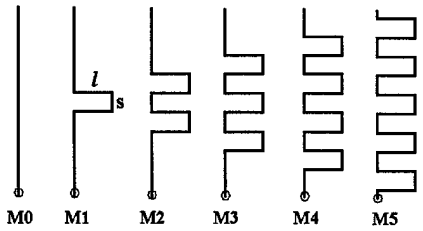

Fig. 1. Meander line antenna geometry.

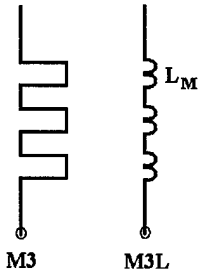

Fig. 2. Equivalent inductor representation of a meander line antenna.

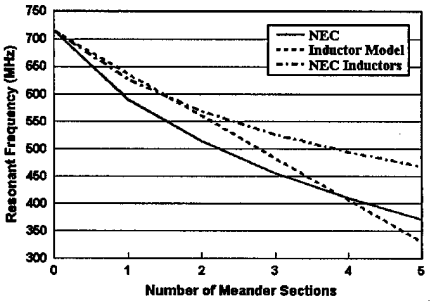

Fig. 3. Resonant frequencies of the meander line antennas, M0 through M5.

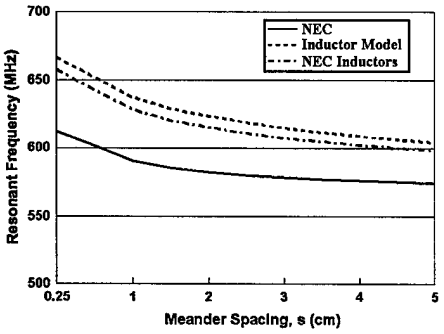

Fig. 4. Resonant frequency as a function of meander spacing.

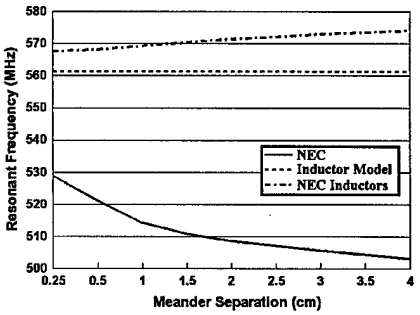

Fig. 5. Resonant frequency as a function of meander separation.

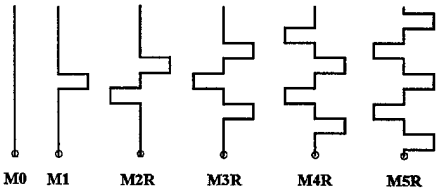

Fig. 6. Meander line antennas with reversed meander sections.

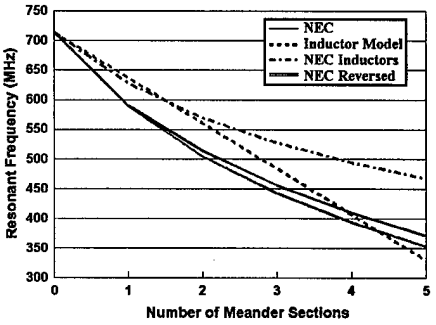

Fig. 7. Resonant frequency of the meander line antennas with reversed meander sections.